NASA Contractor Report 172512

ICASE REPORT NO. 84-61

NASA-CR-172512
19850010354

ICASE

ON THE INTERACTION OF A SOUND PULSE WITH
THE SHEAR LAYER OF AN AXISYMMETRIC JET,
III. NONLINEAR EFFECTS

Alvin Bayliss

Lucio Maestrello

Eli Turkel

INSTITUTE FOR COMPUTER APPLICATIONS IN SCIENCE AND ENGINEERING
NASA Langley Research Center, Hampton, Virginia 23665

Operated by the Universities Space Research Association

NASA

National Aeronautics and
Space Administration

Langley Research Center
Hampton, Virginia 23665

ON THE INTERACTION OF A SOUND PULSE

WITH THE SHEAR LAYER OF AN AXISYMMETRIC JET,

III. NONLINEAR EFFECTS

Alvin Bayliss
Exxon Corporate Research, Clinton, NJ

Lucio Maestrello
NASA Langley Research Center

Eli Turkel
Tel Aviv University, Tel-Aviv, Israel
and
Institute for Computer Applications in Science and Engineering

Abstract

The fluctuating field of a jet excited by transient mass injection is simulated numerically. The model is developed by expanding the state vector as a mean state plus a fluctuating state. Nonlinear terms are not neglected, and the effect of nonlinearity is studied. A high order numerical method is used to compute the solution. The results show a significant spectral broadening in the flow field due to the nonlinearity. In addition, large scale structures are broken down into smaller scales.

N85-18663#

Introduction

This paper deals with a numerical model to simulate a nonlinear inviscid acoustic disturbance in an axisymmetric compressible jet. It also extends previous work on linear acoustic forcing of a jet [1], [2]. Although a true simulation of jet noise should include viscous and three-dimensional effects, the nonlinear effects that we have computed are qualitatively in agreement with observations. These effects include a broadening of the spectrum of the fluctuating field, the breakup of large scale structures and a slowing down of vortex motion. The results show that these effects can be accounted for by nonlinear axisymmetric inviscid interactions.

The method is based on a solution of the Euler equations for homentropic flow in cylindrical coordinates. The jet is excited by transient mass injection. The equations are formulated and solved in conservation form for the fluctuating field, even though we have only computed smooth solutions. In Section 2 we formulate the physical model. In Section 3 we briefly outline the numerical scheme. An extensive description of this scheme can be found in [1]. Numerical results are presented in Section 4, and we discuss some conclusions in Section 5. A preliminary version of these results was presented at the Eighth International Conference on Numerical Methods in Fluid Dynamics (Aachen, 1980 [3]).

2. Physical Model

We consider the Euler equations for a homentropic axisymmetric jet in cylindrical coordinates. The jet is forced by transient, point mass injection. The source strength is scaled by a parameter ε and the state

vector $W = (\bar{p}, \bar{\rho}, \bar{u}, \bar{v})$ is expanded as a mean state plus a fluctuating state of order ε. Here $\bar{p}$ is the pressure, $\bar{\rho}$ the density and $\bar{u}$ and $\bar{v}$ are the axial and radial velocity components respectively.

The solution is expanded in the form $\bar{p} = p_0 + \varepsilon p$, etc. where the mean state (with subscript "0") is assumed to satisfy the unforced Euler equations. The variables (p, ρ, u, v) will represent the fluctuating field in response to the jet forcing. New variables $m = (\rho_0 + \varepsilon \rho)u$ and $n = (\rho_0 + \varepsilon \rho)v$ are introduced for simplicity. With cylindrical spatial coordinates z (axial) and r (radial), the Euler equations for the fluctuating field become

$$\rho_t + \left(\rho U_0 + \rho_0 u\right)_z + \left(\rho V_0 + \rho_0 v\right)_r + \frac{\left(\rho V_0 + \rho_0 v\right)}{r} = M$$

$$m_t + \left(m(U_0 + \varepsilon u)\right)_z + \left(m(V_0 + \varepsilon v)\right)_r + p_z + nU_{0;r} - mV_{0;r} - \frac{\varepsilon nu}{r} = \varepsilon M u \qquad (1)$$

$$n_t + \left(n(U_0 + \varepsilon u)\right)_z + \left(n(V_0 + \varepsilon v)\right)_r + p_r + mU_{0;z} - nV_{0;z} - \frac{\varepsilon nv}{r} = \varepsilon M v,$$

where the subscript r and z stand for differentiation in these variables.

In the development of system (1) one assumes that the derivatives of the mean pressure and density in space can be neglected. This is a consequence of the full Euler equations with a source of mass injection and of the expansion into mean and fluctuating states. The source is εM (units density/time). The mean velocities U_0 and V_0 are taken from measurements of a spreading jet. The system is solved in a cylindrical rectangle including a semi-infinite pipe from which the jet exits. The computational domain is illustrated in Figure 1.

The use of the quasi-momentum variables m and n gives a system for which the fluctuating field can be computed directly rather than as a small

part of the total field. In addition, the linear limit can be recovered by simply setting $\varepsilon = 0$ in (1). The nonlinear terms are explicitly exhibited. The fluctuating pressure p is obtained from the density ρ by the homentropic relation

$$\overline{p} = A\overline{\rho}^{\gamma} = p_0\left(1 + \varepsilon \frac{\rho}{\rho_0}\right)^{\gamma}, \tag{2}$$

where $\gamma = 1.4$ in air.

A fundamental assumption entering into the derivation of (1) is that the mean state is a solution to the unforced Euler equations. This is not true for a state determined from experimental measurements. Numerical experiments have verified, however, that the qualitative features of the fluctuating solution are insensitive to small changes in the mean state; thus we believe that the solution to (1) qualitatively represents the fluctuating field in response to a given source. The use of an experimentally determined meanflow has the advantage that some phenomena not completely governed by the inviscid equations is included in the model.

The source is assumed to be a delta function in space (modelled by a sharp Gaussian) with a pulse-like time dependence. The source location, z_s, is on the jet centerline approximately 1.2 jet diameters downstream of the nozzle exit. Specifically,

$$M(t,z,r) = f(t)\delta\left(r^2 + (z - z_s)^2\right), \tag{3}$$

where the function $f(t)$ is

$$f(t) = e^{-(at^2+bt^{-2})}, \tag{4}$$

for suitable constants a and b.   The use of (4) permits the investigation of a broad band spectrum.

The fluctuating field described by (1) reduces to the acoustic field for large distances.   The near field and flow field are dominated by instability waves which are generated because the mean flow is linearly unstable.   The pulse is assumed to dominate the natural sources of jet noise.   These natural sources are both the linear and nonlinear terms in (1).   In a real jet these terms are determined from the turbulent fluctuations whereas in the numerical model these natural sources are excited by the pulse.   The important physical effect is the generation of packets of instability waves in the flow.   Large scale structures which are related to mean flow instabilities have been observed experimentally in both forced and unforced jets ([4], [5]).   These structures interact with and modify the resulting acoustic fields.   The model permits this interaction to be studied in both the linear ($\epsilon = 0$) and nonlinear ($\epsilon \neq 0$) regimes.   Calculations with the linear model and comparison with experiments are described in [1] and [2].

3. Numerical Model

In this section we discuss the numerical scheme.   The discussion will be brief with the intention of making the paper self-contained.   A more complete discussion can be found in [1].

A numerical simulation of (1), requires the solution to be accurately computed over large length scales.   This necessitates the use of high order accurate discretizations.   The system can be written in the form

$$w_t + F_z + G_r = H,$$

(5)

where w is the vector (ρ, m, n) and F, G, and H are the appropriate vector functions. Equation (5) is split into two one-dimensional operators corresponding to the z and r directions. Each one-dimensional system is integrated by using a fourth-order version of the MacCormack scheme [6]

$$\tilde{w}^{n+1} = w_i^n + \frac{\Delta t}{6\Delta x} \left(-7F_i + 8F_{i+1} - F_{i+2}\right) + \Delta t \tilde{H}_1$$

$$w_i^{n+1} = \frac{1}{2} \left(\tilde{w}^{n+1} + w_i^n + \frac{\Delta t}{6\Delta x} \left(7\tilde{F}_i - 8\tilde{F}_{i-1} + \tilde{F}_{i-2}\right) + \Delta t \tilde{H}_1\right),$$

(6)

together with a symmetric variant interchanging forward and backward differences (H_1 is obtained from some splitting of H). Typical grids require of the order of 40,000 grid points over distances of the order of 50 jet diameters in all directions. Our experience has been that for problems of this size, second-order schemes are not sufficient to obtain accurate solutions using a reasonable amount of computer resources. The explicit scheme (6) naturally lends itself to vectorization and has been implemented on the CDC Cyber-203 with great efficiencies.

In addition, it is necessary to impose boundary conditions which accurately simulate outgoing radiation at the far field boundaries. A family of radiation boundary conditions has been developed which provide increasingly accurate approximations to outgoing radiation. The leading member of this family is

$$p_t + \rho_\infty c_\infty \tilde{u}_t + \frac{p}{d} = 0,$$

(7)

where c_∞ is the ambient sound speed and ρ_∞ the ambient density [1]. Here $d^2 = r^2 + z^2$ and $\tilde{u}$ is the outgoing radial velocity based on a spherical coordinate system near the source.

System (1) includes terms proportional to r^{-1}. This singularity at the axis is resolved using L'Hospital's rule and including these terms in the flux vector G when r = 0. In addition, it is necessary to modify the difference formula (6) at boundaries. This is accomplished by introducing fictitious grid points outside of the computational domain and using a third-order extrapolation of the flux function (F or G). This approach was found to be the most readily vectorizable. It has been verified that the resulting scheme is fourth-order accurate.

4. Results

We next describe results illustrating the effect of the nonlinear terms on the fluctuating field. In Figures 2, 3 and 4 the fluctuating pressure is shown as a function of axial location z/D (D is the jet diameter) and non-dimensional time tc_∞/D for three different radial positions and for $\varepsilon = 0.00$ and $\varepsilon = 0.05$. All figures show an acoustic wave (speed of sound normalized to unity) in the downstream direction trailed by several much larger waves. These are instability waves which travel with a speed of approximately $.7U_j$ where $U_j = .66c_\infty$ is the jet exit velocity. A series of acoustic ripples can also be seen propagating upstream. These are due to diffraction of the upstream acoustic wave by the nozzle lip.

The figures indicate that the nonlinear terms have little effect on the primary acoustic pulse and on the acoustic diffraction from the nozzle lip. The nonlinearity has a pronounced effect on the instability waves. Increasing the nonlinearity causes these predominantly large scale structures to break up into smaller scale structures. This can be seen in both the additional ripples which trail the instability waves and a sharpening of the individual

pulses indicating an enhanced high frequency content. It is also evident that for increasing r/D, these smaller scale structures are comparable in amplitude to the primary instability waves. We observe that the structure of the linear solution changes gradually as r/D increases, whereas the nonlinear solution is much more sensitive to the radial position, with the most pronounced effects on the jet centerline.

In Figure 5 the fluctuating pressure at a point in the flow is plotted as a function of tc_∞/D for three different values of ϵ. It is apparent that the acoustic wave (earliest arrival) is completely unaffected by the nonlinearity. The later arrival (instability wave) is significantly affected. For a weak nonlinearity ($\epsilon = 0.025$) the waveform is not changed but the large negative peak is sharpened and enhanced at the expense of the other peaks. For a large nonlinearity ($\epsilon = 0.05$) there is a pronounced breakdown of the waveform indicating a generation of smaller scale structures.

In Figure 6, the fluctuating vorticity is shown for three different values of ϵ at an early time ($tc_\infty/D = 10$). The intense vortices correspond to the instability waves. Increasing ϵ causes the vorticity to concentrate near the jet centerline. This is consistent with observations in real jets downstream of the potential core. Increasing the nonlinearity also tends to reduce the convective speed of the vortices. Thus the trailing vortices catch up with the leading vortices. In Figure 7 the fluctuating vorticity is shown for a later time ($tc_\infty/D = 30$) where there is a residual shedding of vorticity from the nozzle lip. A possible pairing of vortices can be observed. True vortex merging, which has been observed experimentally [7] depends heavily on viscosity as well as nonlinearity and is not simulated in this model.

In Figures 8a-8c the normalized power spectral densities (PSD) for the fluctuating axial velocity are plotted as a function of Helmholtz number fD/U_j, where f is the frequency, for $\varepsilon = 0.0$ and $\varepsilon = 0.05$. The figures are taken at a fixed axial location ($z/D = 7.3$) and for three different radial locations. The figures clearly indicate a shift into higher frequencies and an overall broadening of the spectra. The PSD for the nonlinear case is highly sensitive to radial position, again indicating a breakdown of the fluctuating field into smaller scales.

In Figures 9a and 9b the PSD for the fluctuating pressure is shown for two farfield angles. The data at $\theta = 27.8^{\circ}$ from the jet axis clearly exhibits a spectral broadening and thus indicates that nonlinear effects can be transmitted to the farfield. In Figure 9b the results are shown at $\theta = 90^{\circ}$. There is virtually no effect of the nonlinearity at higher angles. For the linear case, we have found that the acoustic field resulting from the large scale structures mostly affects angles around 30° (see [1]) and we believe that the nonlinear effects in Figure 9a are due to the breakdown of the large scale structures in the near field.

5. Discussion

The fundamental difference between the nonlinear and linear computations is the breakdown of the large scale structures into smaller scale structures in the nonlinear case. This is associated with a transfer of energy into higher frequencies or equivalently a broadening of the spectral content of the fluctuating field. It is also illustrated by the increased interaction between the different vortices. In real jets this is a fundamental step in the transition to fully-developed turbulence. The results clearly indicate

that at least the initial stages of this energy cascade into smaller scales can be simulated just by the nonlinear terms of an axisymmetric and inviscid calculation.

In previous papers (see [1], [2]) the authors have demonstrated a close connection between the far field acoustic pressure and near field large scale structures (instability waves). The present results (in particular, Figure 9a) demonstrate that the far field spectrum can also be sensitive to nonlinearities which predominate in the near field. These results demonstrate that far field jet acoustic phenomena are inextricably connected to the fluid dynamics of the jet. Therefore, in order to analyze and interpret jet acoustic phenomena it may be necessary to employ the full nonlinear equations of fluid dynamics.

In [1], [2] the authors demonstrated that a fourth-order accurate scheme was necessary in order to compute the acoustic far field. This was because the solution had to be computed over many wavelengths. The computations would not have been feasible with a second-order scheme. The solution of the nonlinear equations requires still more resolution because of the generation of smaller scale fluctuations by the nonlinear terms. The computational difficulties in this problem are typical of many other problems involving wave propagation, reflection, and interactions (e.g., elastodynamics, electromagnetism, and general acoustic phenomena). The results indicate that higher order schemes are essential for the effective computation of a wide variety of wave phenomena.

References

[1] Maestrello, L., A. Bayliss, and E. Turkel: "On the interaction of a sound pulse with the shear layer of an axisymmetric jet," J. Sound & Vib., Vol. 74, 1981, pp. 281-301.

[2] Bayliss, A. and L. Maestrello: "On the interaction of a sound pulse with the shear layer of an axisymmetric jet, II. Heated Jets," J. Sound & Vib., Vol. 86, 1982, pp. 395-409.

[3] Bayliss, A., L. Maestrello and E. Turkel: "Simulation of the fluctuating field of a forced jet," Proc. Eight Intl. Conference on Numerical Methods in Fluid Dynamics, Springer-Verlag Lecture Notes in Physics, Vol. 179, 1982, pp. 131-137.

[4] Crow, S. C . and F. H. Champagne: "Orderly structure in jet turbulence," J. Fluid Mech., Vol. 48, Part 3, 1971, pp. 547-591.

[5] Maestrello, L. and Y. T. Fung: "Quasi-periodic structure of a turbulent jet," J. Sound & Vib., Vol. 64, 1979, pp. 107-122.

[6] Gottlieb, D. and E. Turkel: "Dissipative two-four methods for time-dependent problems, Math. Comp., Vol. 30, 1976, pp. 703-723.

[7] Ho, Chi-ming and Lein-saing Huang: "Subharmonics and vortex merging in mixing layers," J. Fluid Mech., Vol. 119, 1982, pp. 443-473.
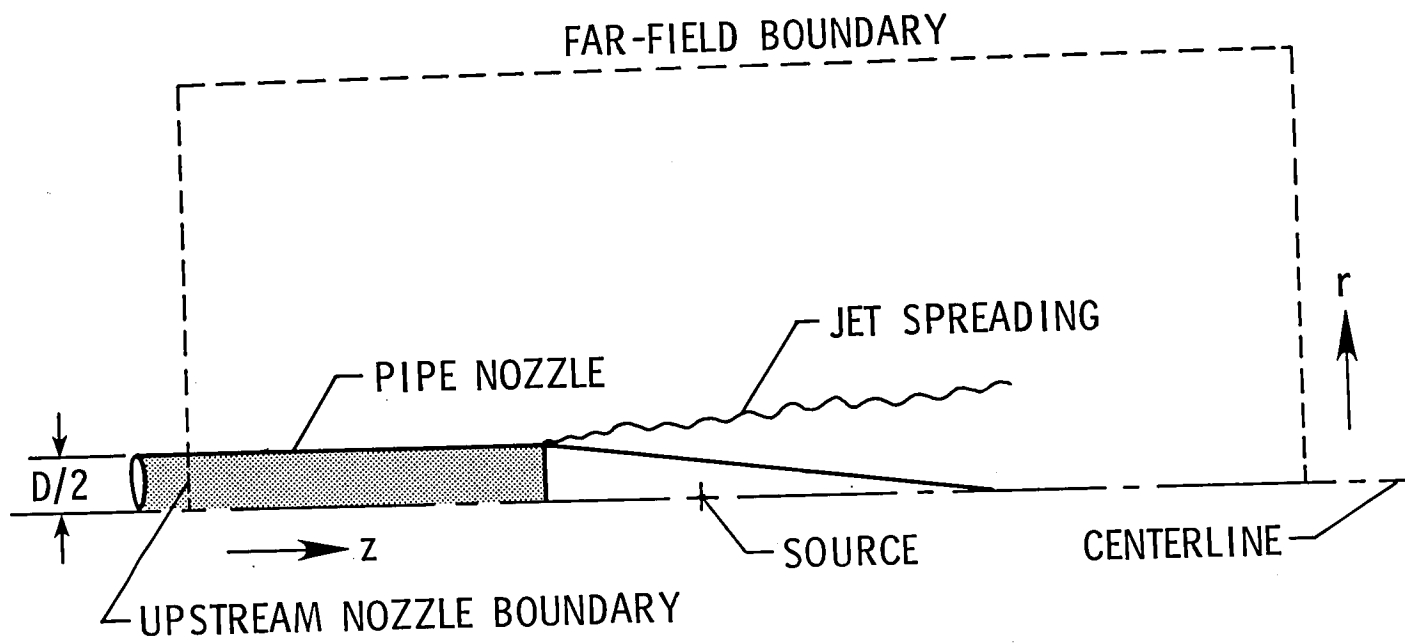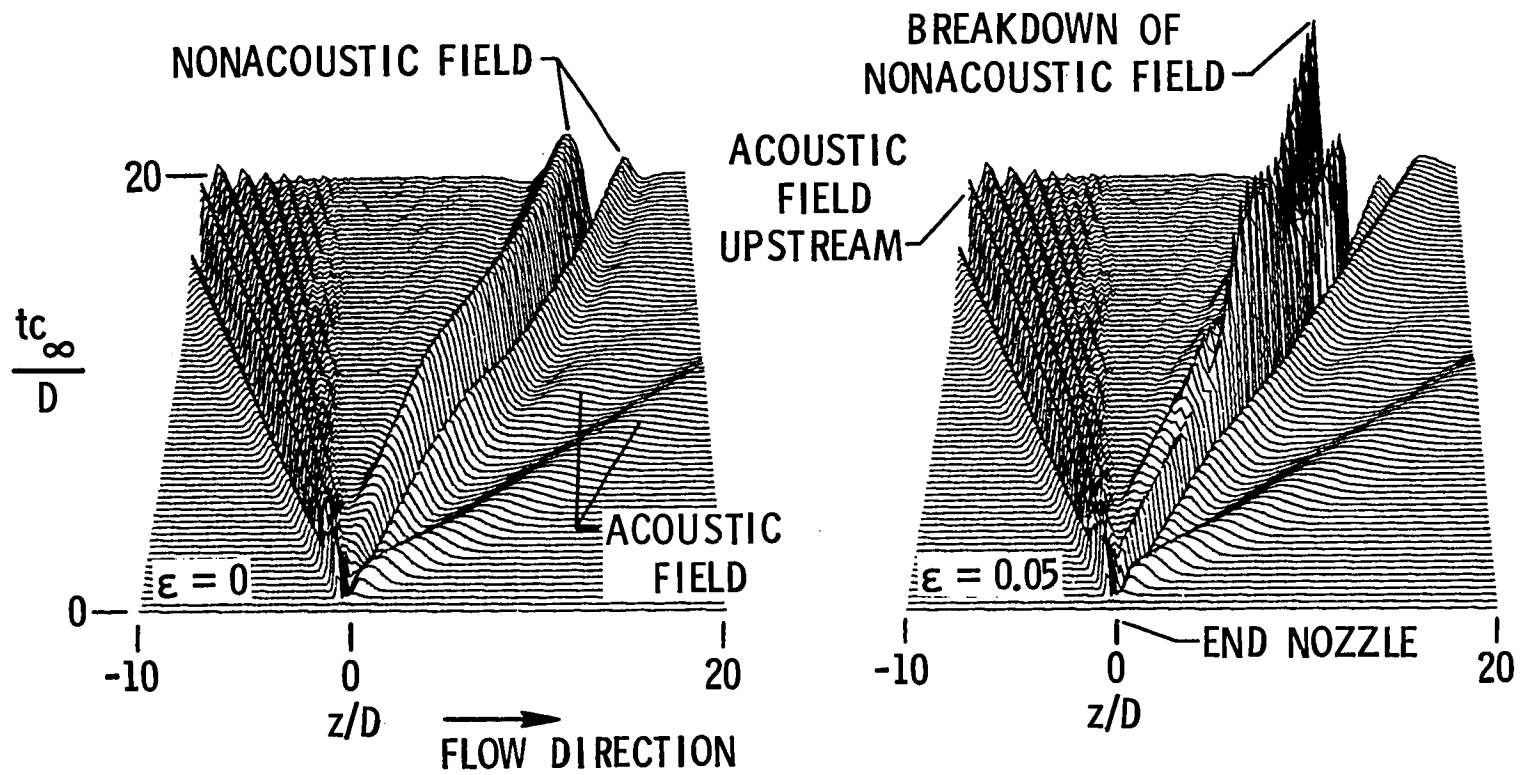
Figure 1. Computational Domain

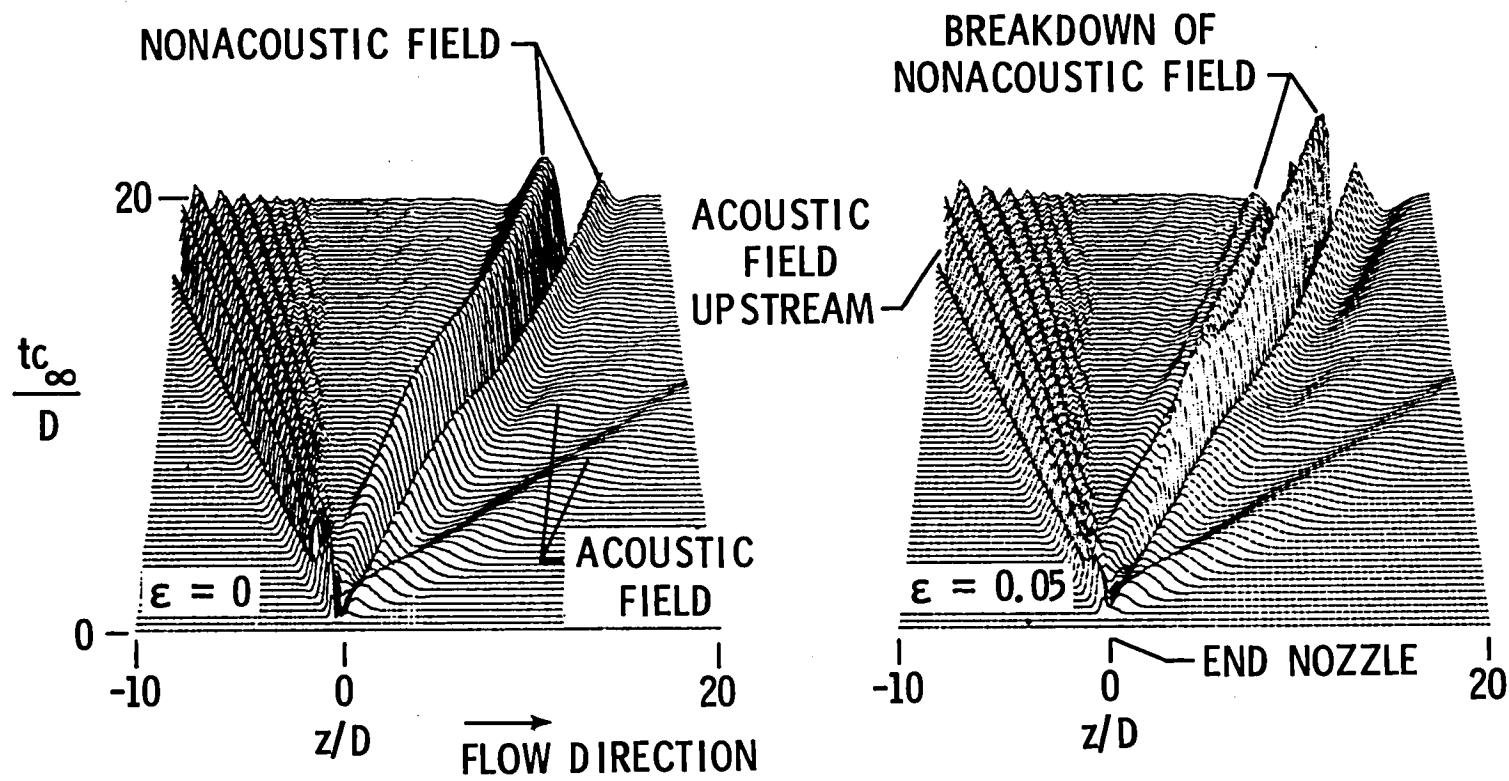Figure 2. Three-dimensional Plots of the Fluctuating Pressure   r/D = 0.0.

NONACOUSTIC FIELD

BREAKDOWN OF
NONACOUSTIC FIELD

$\dfrac{tc_\infty}{D}$

20

ACOUSTIC
FIELD
UPSTREAM

$\varepsilon = 0$

ACOUSTIC
FIELD

$\varepsilon = 0.05$

0

-10   0   20
z/D   FLOW DIRECTION

END NOZZLE

-10   0   20
z/D

Figure 3. Three-dimensional Plots of the Fluctuating Pressure r/D = .29.

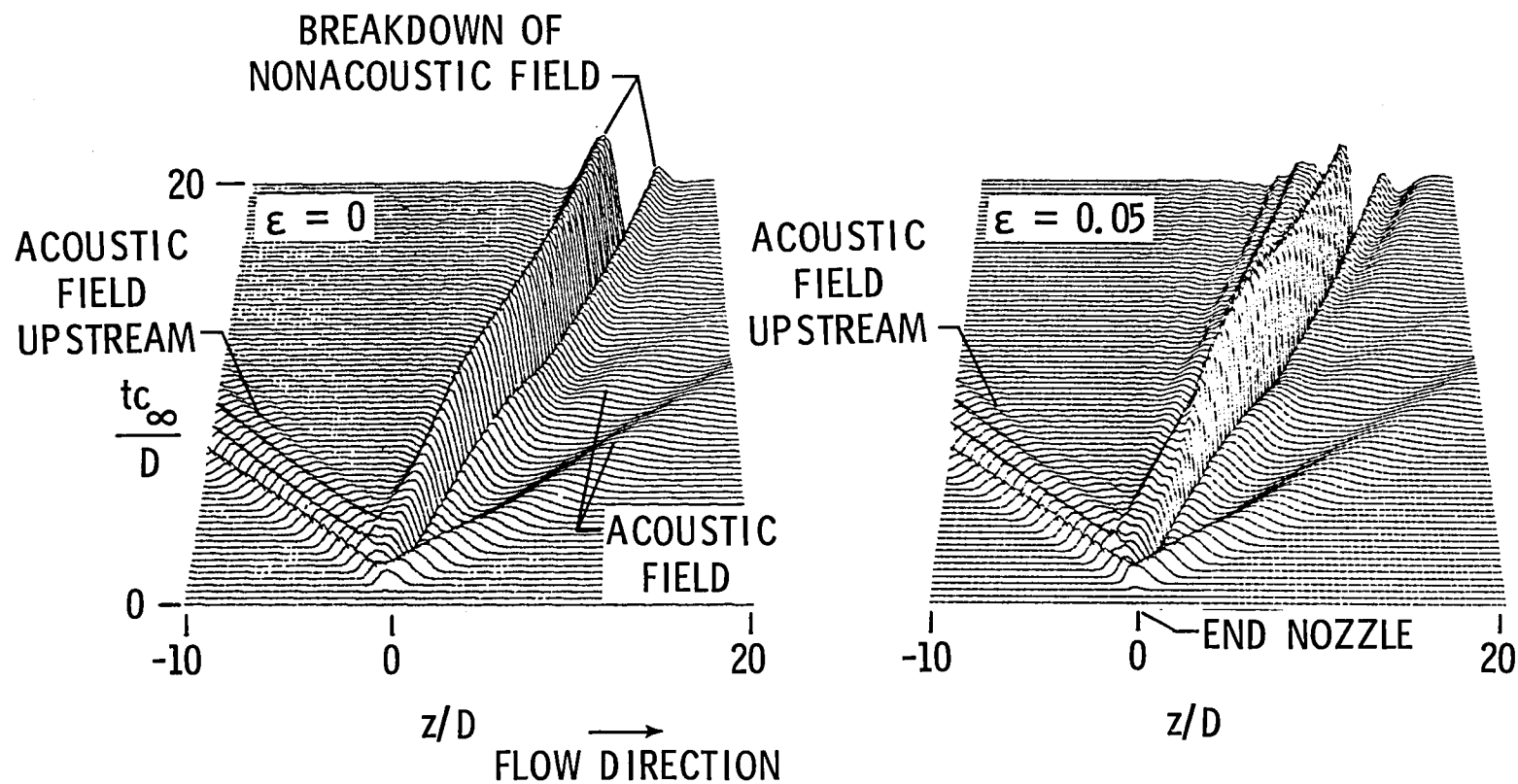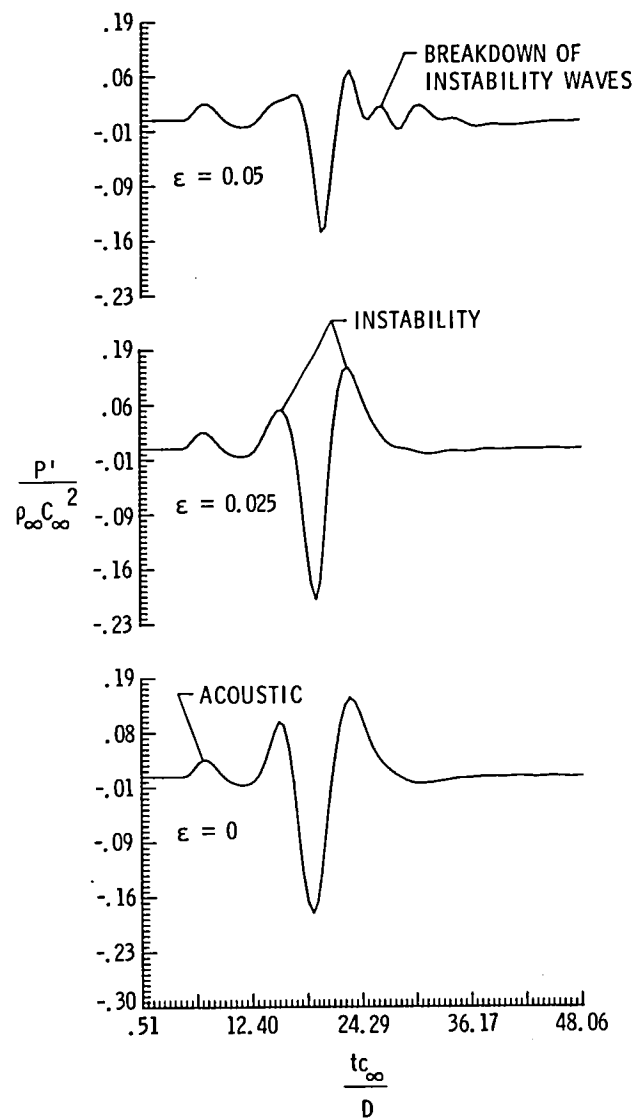Figure 4. Three-dimensional Plots of the Fluctuating Pressure r/D = 0.61.

Figure 5. Fluctuating Pressure z/D = 8.0, r/D = 0.29.
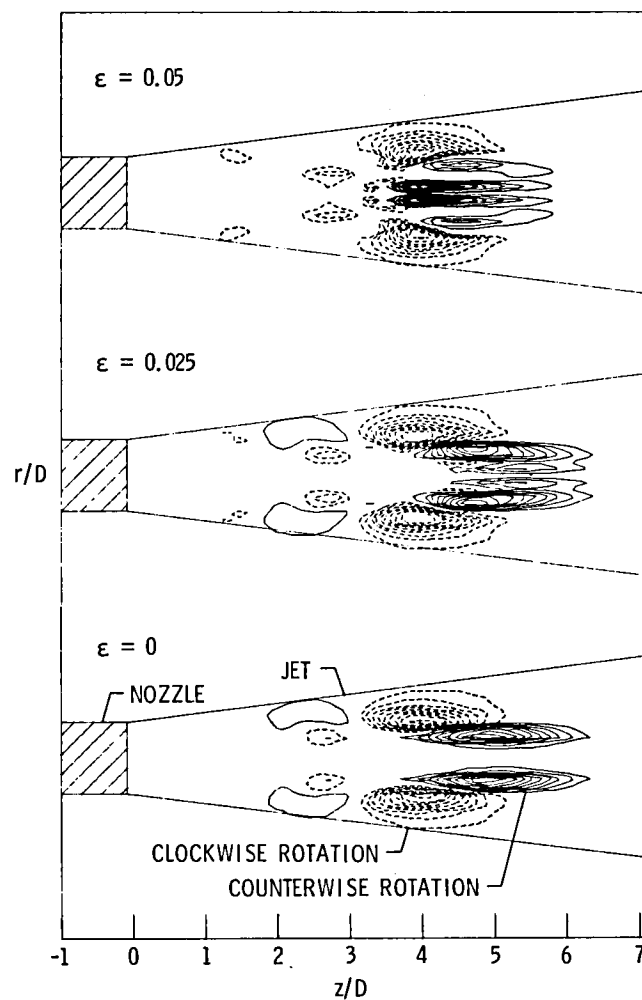
Figure 6. Fluctuating Vorticity $tc_\infty/D = 10$.
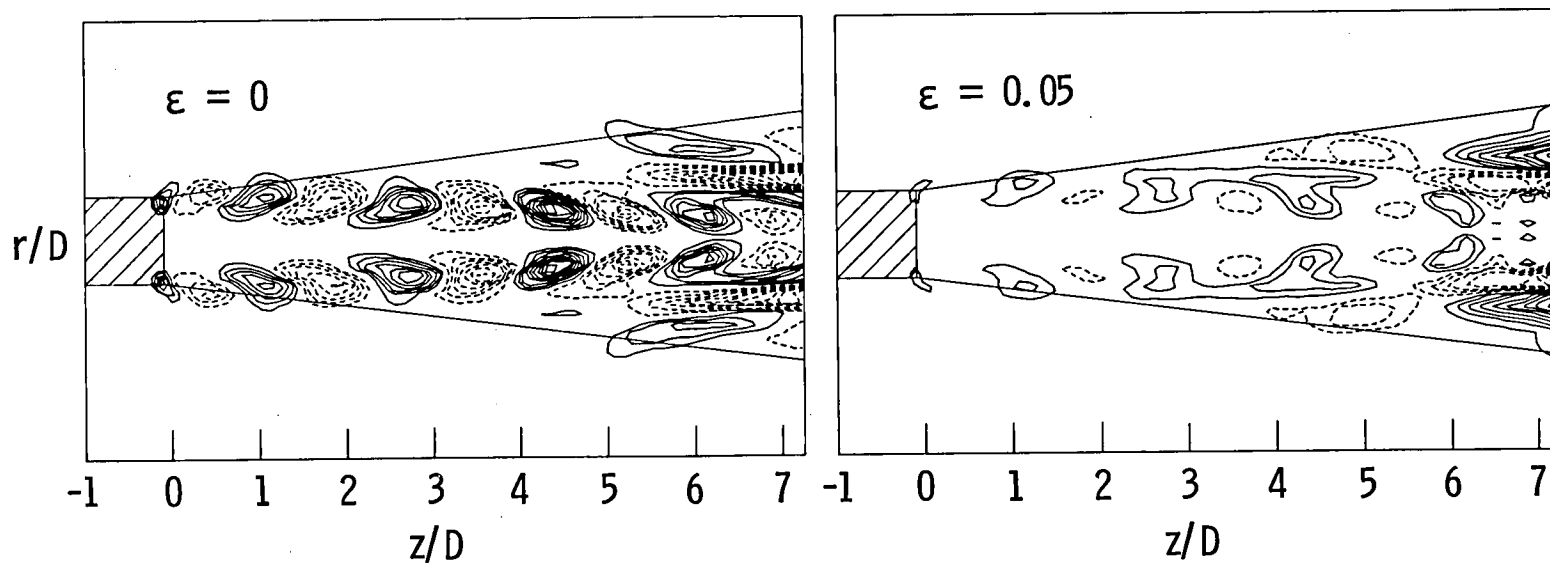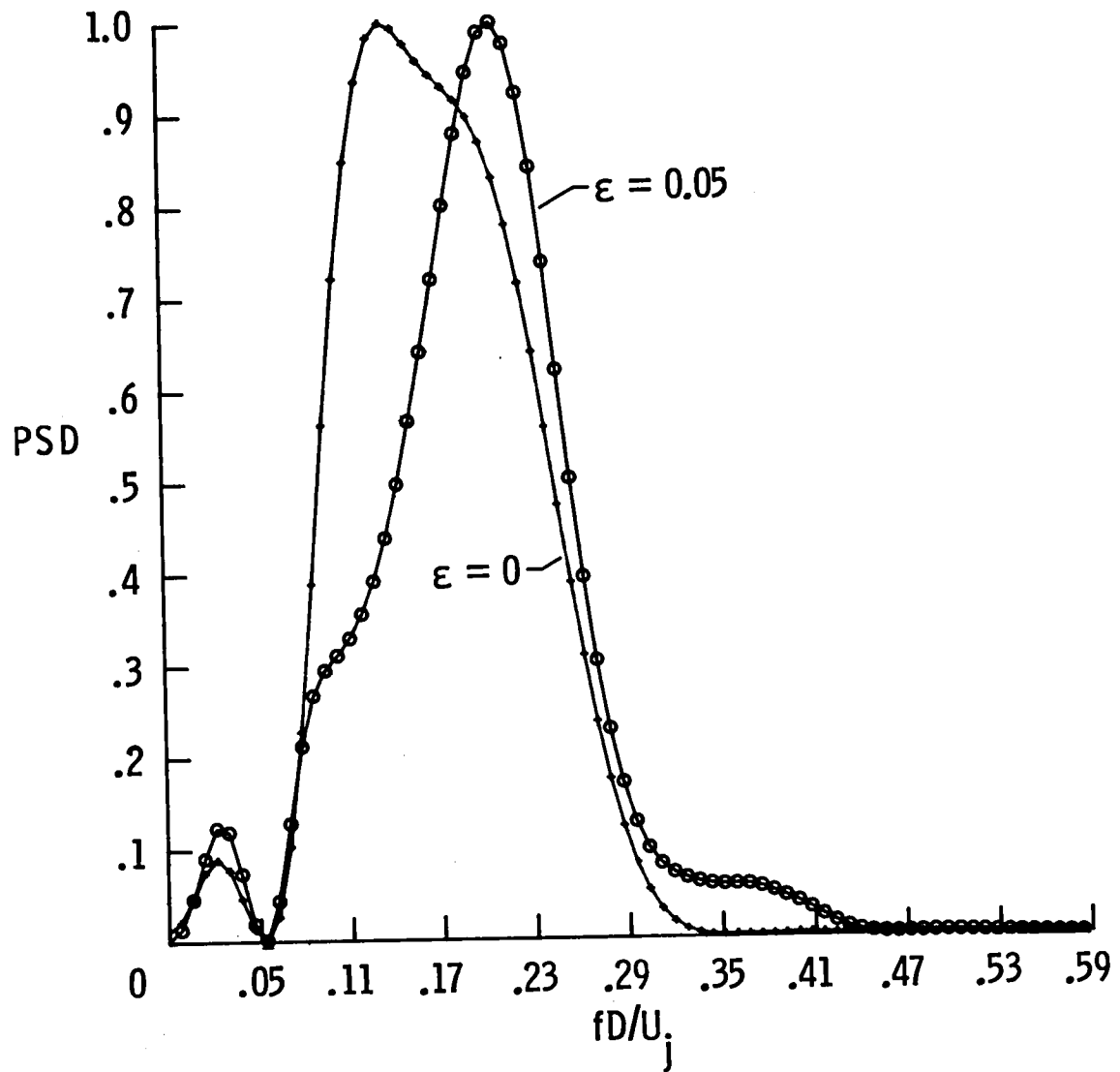
Figure 7.   Fluctuating Vorticity at $tc_\infty/D = 30$.

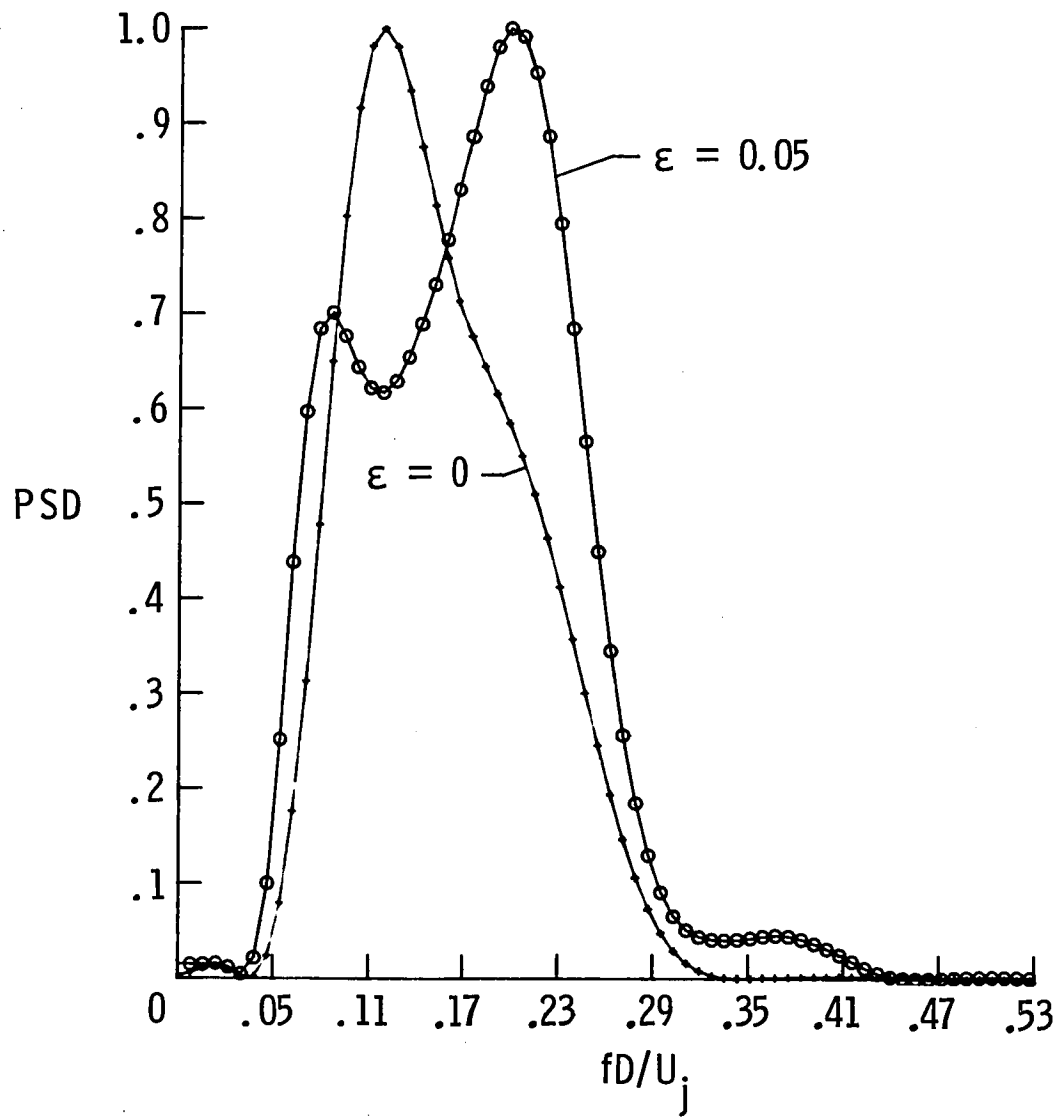Figure 8a. Flow Field Velocity Spectra z/D = 7.3 , r/D = 1.3.

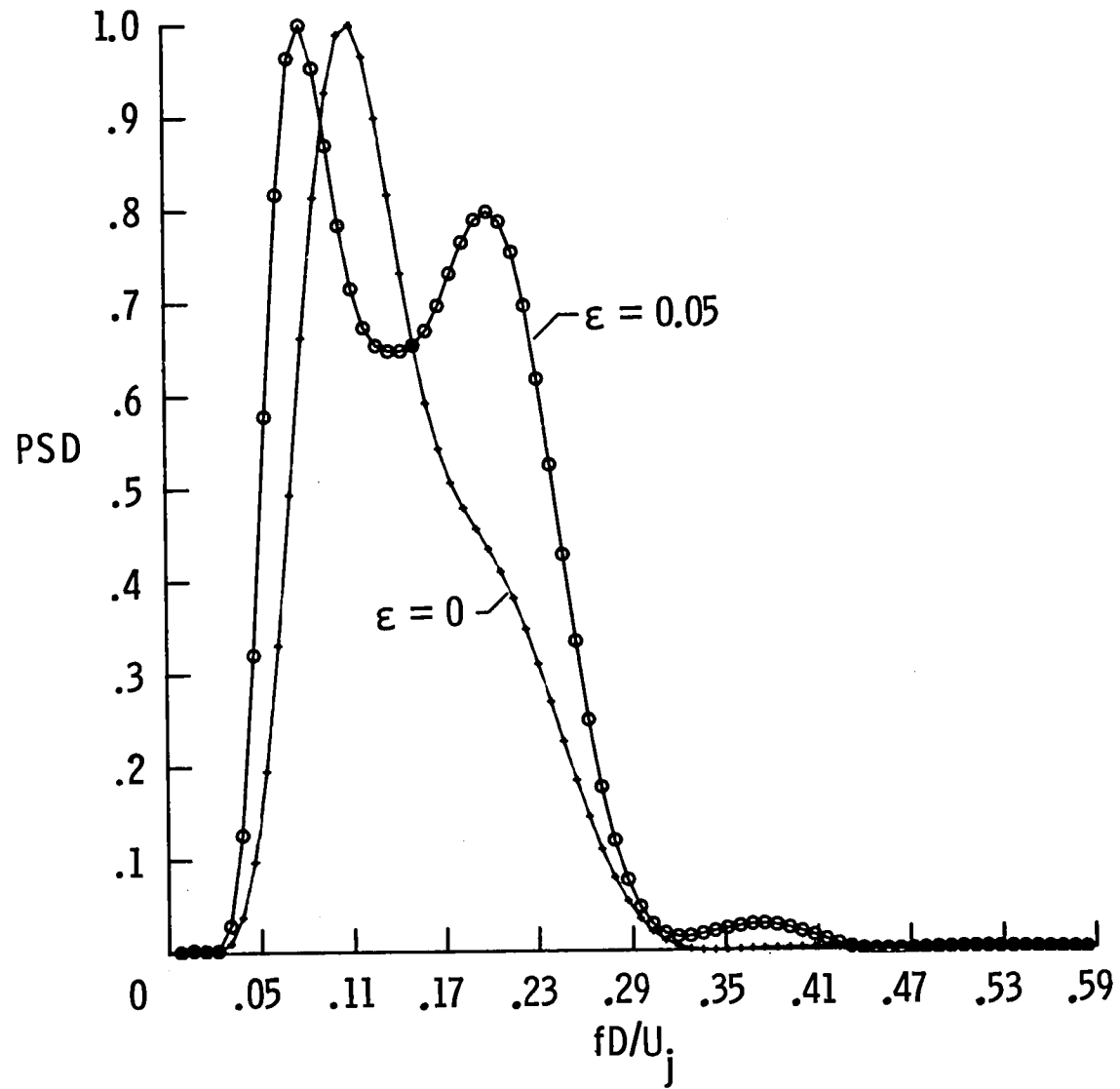Figure 8b.   Flow Field Velocity Spectra   z/D = 7.3, r/D 1.5.

Figure 8c.   Flow Field Velocity Spectra   z/D = 7.3, r/D = 1.7.
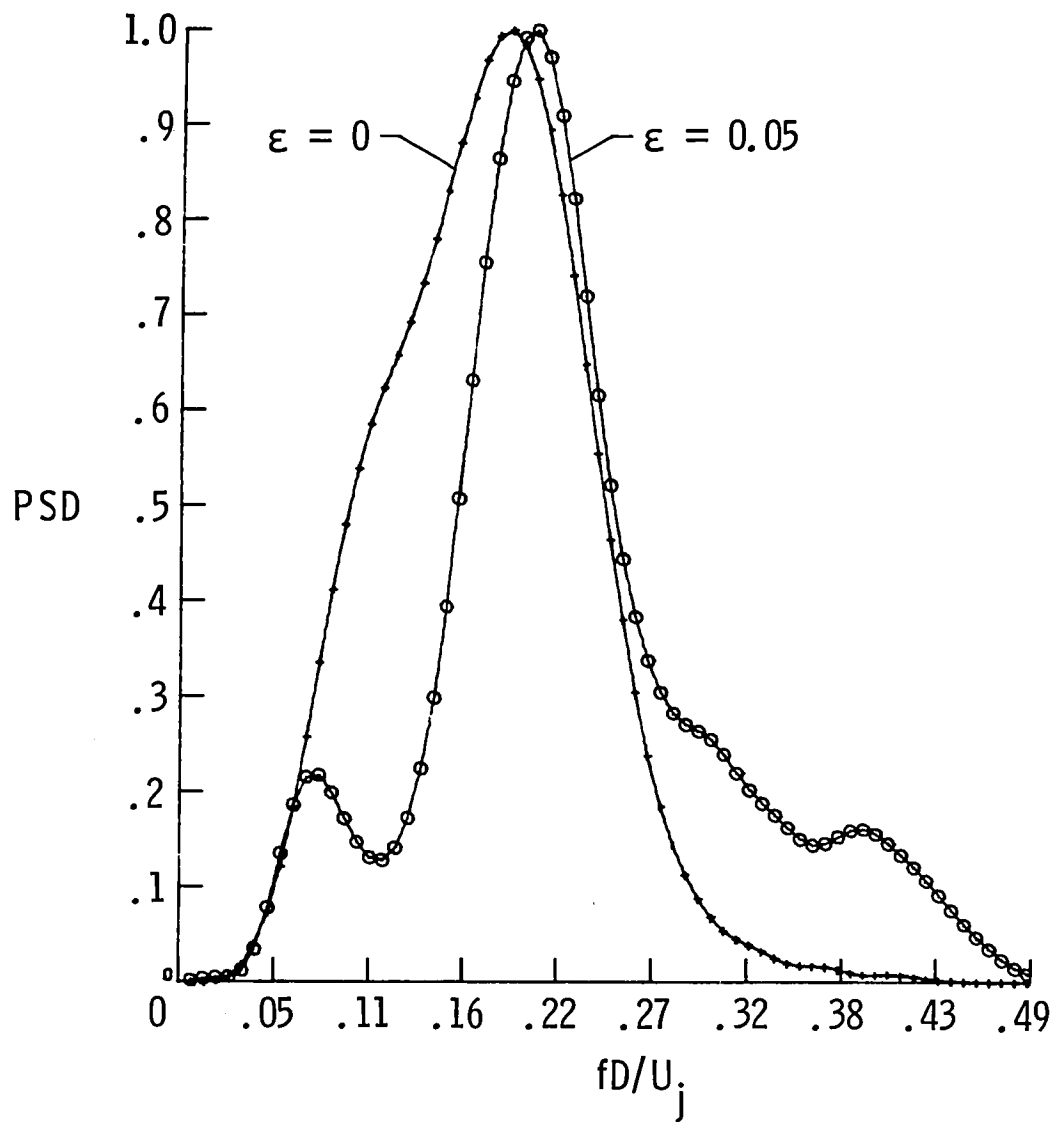
Figure 9a. Acoustic Far Field Spectra z/D = 37, θ = 27.8°.
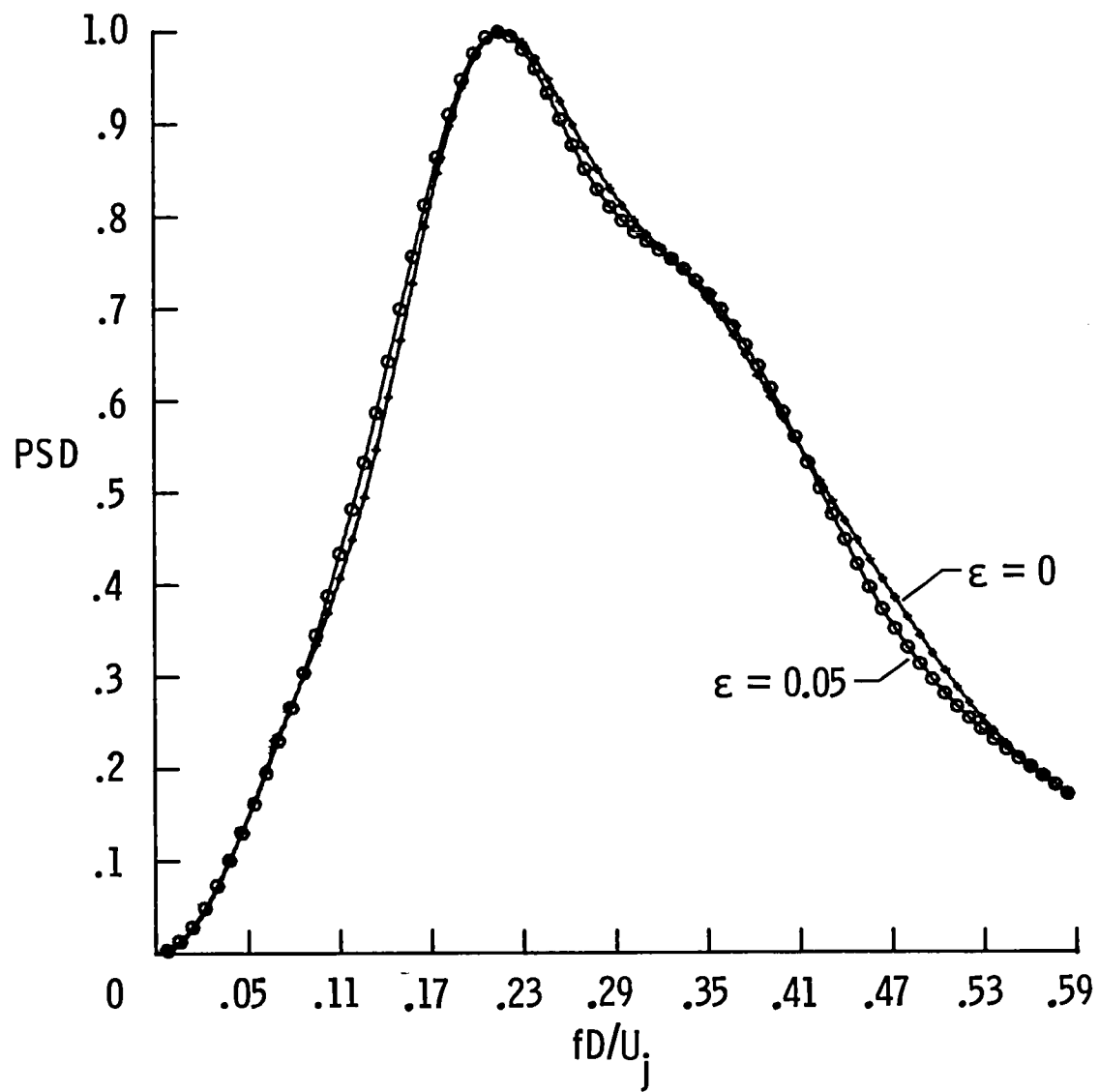
Figure 9b. Acoustic Far Field Spectra z/D = 38, $\theta = 90^{\circ}$.

1. Report No. NASA CR-172512 ICASE Report No. 84-61	2. Government Accession No.	3. Recipient's Catalog No.
4. Title and Subtitle ON THE INTERACTION OF A SOUND PULSE WITH THE SHEAR LAYER OF AN AXISYMMETRIC JET, III. NONLINEAR EFFECTS		5. Report Date January 1985
		6. Performing Organization Code
7. Author(s) Alvin Bayliss, Lucio Maestrello, and Eli Turkel		8. Performing Organization Report No. 84-61
		10. Work Unit No.
9. Performing Organization Name and Address Institute for Computer Applications in Science and Engineering Mail Stop 132C, NASA Langley Research Center Hampton, VA 23665		11. Contract or Grant No. NAS1-15810; 16394; 17130; and 17170
		13. Type of Report and Period Covered Contractor Report
12. Sponsoring Agency Name and Address National Aeronautics and Space Administration Washington, D.C. 20546		14. Sponsoring Agency Code 505-31-83-01

15. Supplementary Notes
Langley Technical Monitor: J. C. South, Jr. Final Report

16. Abstract

The fluctuating field of a jet excited by transient mass injection is simulated numerically. The model is developed by expanding the state vector as a mean state plus a fluctuating state. Nonlinear terms are not neglected, and the effect of nonlinearity is studied. A high order numerical method is used to compute the solution. The results show a significant spectral broadening in the flow field due to the nonlinearity. In addition, large scale structures are broken down into smaller scales.

17. Key Words (Suggested by Author(s)) acoustics, nonlinearities, high order schemes	18. Distribution Statement 64 - Numerical Analysis 71 - Acoustics Unclassified - Unlimited	
19. Security Classif. (of this report) Unclassified	20. Security Classif. (of this page) Unclassified	21. No. of Pages 23	22. Price A02